doi:10.1016/j.jmb.2010.10.020 J. Mol. Biol. (2011) 405, 666–678

Contents lists available at www.sciencedirect.com

Journal of Molecular Biology

journal homepage: http://ees.elsevier.com.jmb

Fluorescence-Based Assay to Measure the Real-time Kinetics of Nucleotide Incorporation during Transcription Elongation

Guo-Qing Tang, Vasanti S. Anand and Smita S. Patel*

Department of Biochemistry, Robert Wood Johnson Medical School, University of Medicine and Dentistry of New Jersey, 683 Hoes Lane, Piscataway, NJ 08854, USA

Received 28 July 2010;
received in revised form
14 October 2010;
accepted 14 October 2010
Available online
28 October 2010

Edited by R. Ebright

Keywords:
2-aminopurine fluorescence;
real-time kinetics;
single-nucleotide incorporation;
T7 RNA polymerase;
transcription elongation

Understanding the mechanism and fidelity of transcription by the RNA polymerase (RNAP) requires measurement of the dissociation constant (K_d) of correct and incorrect NTPs and their incorporation rate constants (k_{pol}). Currently, such parameters are obtained from radiometric-based assays that are both tedious and discontinuous. Here, we report a fluorescence-based assay for measuring the real-time kinetics of single-nucleotide incorporation during transcription elongation. The fluorescent adenine analogue 2-aminopurine was incorporated at various single positions in the template or the nontemplate strand of the promoter-free elongation substrate. On addition of the correct NTP to the T7 RNAP-DNA, 2-aminopurine fluorescence increased rapidly and exponentially with a rate constant similar to the RNA extension rate obtained from the radiometric assay. The fluorescence stopped-flow assay, therefore, provides a high-throughput way to measure the kinetic parameters of RNA synthesis. Using this assay, we report the k_{pol} and K_d of all four correct NTP additions by T7 RNAP, which showed a range of values of 145–190 s^{-1} and 28–124 μM, respectively. The fluorescent elongation substrates were used to determine the misincorporation kinetics as well, which showed that T7 RNAP discriminates against incorrect NTP both at the nucleotide binding and incorporation steps. The fluorescence-based assay should be generally applicable to all DNA-dependent RNAPs, as they use similar elongation substrates. It can be used to elucidate the mechanism, fidelity, and sequence dependency of transcription and is a rapid means to screen for inhibitors of RNAPs for therapeutic purposes.

Introduction

Transcription is catalyzed by the DNA-dependent RNA polymerase (RNAP) in two stages: initiation and elongation. During the initiation phase, the RNAP binds to a specific promoter sequence on the genomic DNA to initiate *de novo* RNA synthesis from NTPs. This initial phase of transcription is slow, nonprocessive, and characterized by the production of abundant short abortive RNA products.[1–4] RNA synthesis becomes fast and processive after 9- to 12-nt RNA synthesis, when the RNAP escapes the promoter to enter into the elongation phase.[4–6] For accurate and timely gene expression, it is crucial that the RNAP transcribes the genomic DNA with high fidelity and makes the RNA message efficiently. To measure the fidelity

*Corresponding author. E-mail address: patelss@umdnj.edu.

Abbreviations used: RNAP, RNA polymerase; GTP, guanosine 5′-triphosphate; 2AP, 2-aminopurine; 3′-dC, 3′-deoxycytidine; T, template; NT, nontemplate.

and efficiency of RNA synthesis, it is necessary to determine the single-nucleotide incorporation rate constants using pre-steady-state kinetic methods. Compared to the wealth of information on the transient kinetic mechanism and fidelity of DNA synthesis,[7–10] there are only a few kinetic measurements of the RNAPs that provide the fundamental knowledge to assess the efficiency and fidelity of the transcription reaction.[11–14]

Kinetic studies of RNA synthesis during the elongation phase have been hampered by the necessity to go through the initiation steps at the promoter.[15] Since transcription initiation is slow and nonprocessive, the reaction becomes asynchronous by the time the RNAP reaches elongation. This problem has been overcome by the discovery that RNAPs can bind to promoter-free RNA:DNA hybrid substrates that support RNA elongation with high efficiency.[16–21] Biochemical studies including crystal structures have shown that the single subunit T7 RNAP binds to the promoter-free RNA:DNA elongation substrate in its transformed elongation conformational state.[13,16–18] The promoter-free RNA:DNA serves as an efficient elongation substrate to quantitatively measure the elementary rate constants of UTP addition by T7 RNAP.[13]

Thus far, kinetic measurements of RNA elongation have been carried out using a radiolabeled RNA and by monitoring its elongation using rapid chemical quenched-flow methods.[11–14] Although the radiometric assay is robust, it is tedious and measures RNA synthesis in a discontinuous manner, which is not conducive to high-throughput analysis of enzyme kinetics. A real-time fluorescence-based assay with the ability to measure the kinetics of single-nucleotide addition would overcome these limitations of the radiometric assay and facilitate in-depth studies of the mechanism and fidelity of transcription under various DNA sequence contexts and reaction conditions. Currently, there are no high-throughput assays to measure the kinetics of single-nucleotide incorporation by RNAPs.

In this study, we report a fluorescence-based assay to measure the kinetics of single-nucleotide addition by T7 RNAP based on 2-aminopurine (2AP) fluorescence. The 2AP is a fluorescent base analogue of adenine that can form two hydrogen bonds with thymine or uridine with minimal interference to the duplex DNA stability (Fig. 1a). The fluorescence of 2AP is sensitive to base-stacking interactions with the neighboring bases, a property used extensively to quantify the kinetics and thermodynamics of open

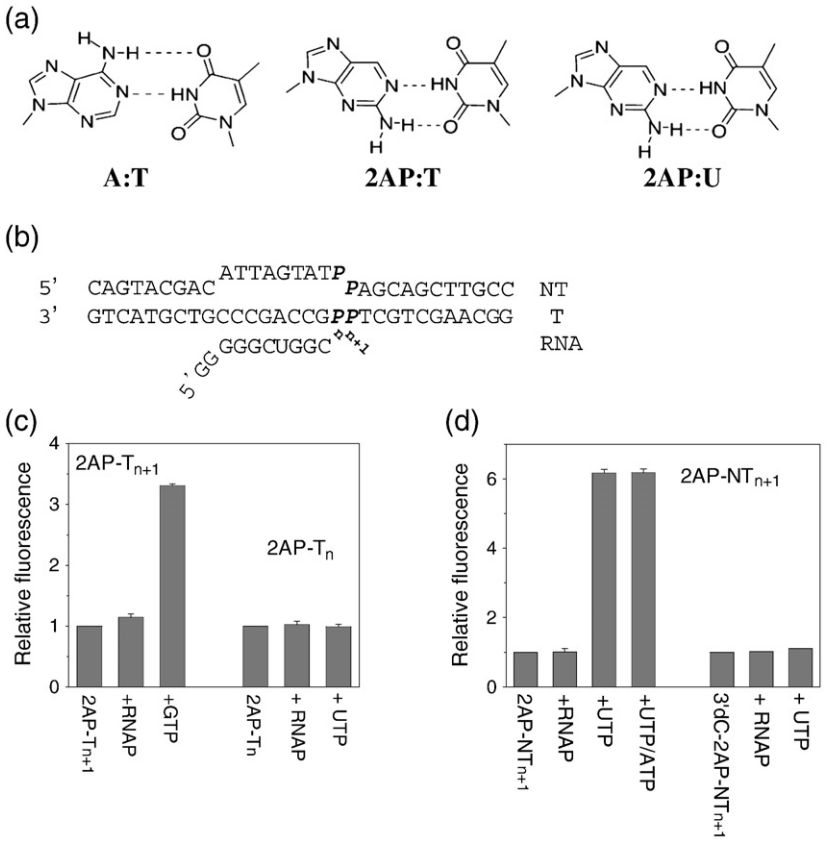

Fig. 1. 2-Aminopurine modifies elongation substrates and their fluorescence properties with and without T7 RNAP and NTP. (a) A:T base pair compared to 2AP:T and 2AP:U base pairs. (b) The elongation substrate showing the positions where a single 2AP was incorporated (denoted as ***P***). (c) 2AP fluorescence was collected over 360–400 nm with excitation at 310 nm and the intensity was normalized to that of individual 2AP-containing elongation substrate. Relative fluorescence is shown for substrates alone with 2AP at T_{n+1} or T_n (200 nM C/2AP-T_{n+1} or 2AP/2AP-T_n), with T7 RNAP (400 nM), and with RNAP and the next correct NTP (400 μM). (d) Relative fluorescence of substrate with 2AP at NT_{n+1} (200 nM A/2AP-NT_{n+1}), with T7 RNAP, and with RNAP and UTP, UTP + ATP, or the incorrect CTP (400 μM each). 3′-dC-SC1A contains a 3′-deoxyCMP (3′-dC) base at the 3′ terminus of the RNA primer.

complex formation by RNAP during initiation[14,22–24] and to measure the kinetics of nucleotide addition by DNA polymerases.[25–29] A previous study has shown that a pair of 2AP placed in the elongation substrate can report on the RNA elongation reaction by T7 RNAP.[30] Here, we have investigated if a single 2AP placed at an appropriate position in the elongation substrate can monitor the kinetics of RNA elongation by one nucleotide. To find the site for 2AP incorporation that is most sensitive to the RNA synthesis step, we investigated several elongation substrates where a single 2AP was placed at a defined position around the NMP incorporation site. Using this approach, we have identified elongation substrates that serve as fluorogenic substrates for investigating the kinetics of RNAP-catalyzed transcription elongation in real time. Since single- and multi-subunit RNAPs use similar elongation substrates to catalyze RNA elongation,[16,19,20,31,32] it is likely that these substrates will serve as general fluorogenic elongation substrates for high-throughput screening of inhibitors and regulators of the RNAPs.

Results

Substrate design for the fluorescence-based elongation assay

A minimal promoter-free elongation substrate was made by annealing two DNA strands to create a preformed 9-bp bubble to which a short RNA was annealed (Table 1; Fig. 1b). A single 2AP was placed either in the template (T) or in the nontemplate (NT) strand at selected positions. In the T strand, the 2AP was placed at the *n*-position (where the incoming NTP base-pairs; T_n) or in the $n+1$ position (T_{n+1}). In the NT strand, 2AP was placed in the position complementary to T_n or T_{n+1} (NT_n or NT_{n+1}, respectively).

Table 1. Sequences of the elongation substrates with 2AP substitution

Elongation substrate[a]	Sequences (RNA with a GG overhang)	Incoming correct NTP
2AP/2AP-T_n	ATTAGTATC 5′CAGTACGAC AAGCAGCTTGCC NT 3′GTCATGCTGCCCGACCG***P***TTCGTCGAACGG T GGGCUGGC[n] RNA 5′GG	UTP
C/2AP-T_{n+1}	ATTAGTATC 5′CAGTACGAC TAGCAGCTTGCC NT 3′GTCATGCTGCCCGACCGC***P***TCGTCGAACGG T GGGCUGGC[n+1] RNA 5′GG	GTP
T/2AP-T_{n+1}	ATTAGTATC 5′CAGTACGAC TAGCAGCTTGCC NT 3′GTCATGCTGCCCGACCGT***P***TCGTCGAACGG T GGGCUGGC[n+1] RNA 5′GG	ATP
G/2AP-NT_n	ATTAGTAT***P*** 5′CAGTACGAC[n] AGCAGCTTGCCA NT 3′GTCATGCTGCCCGACCGGTCGTCGAACGGT T GGGCUGGC RNA 5′GG	CTP
A/2AP-NT_{n+1}	ATTAGTATC[n+1] 5′CAGTACGAC ***P***AGCAGCTTGCC NT 3′GTCATGCTGCCCGACCGATTCGTCGAACGG T GGGCUGGC RNA 5′GG	UTP
A/2AP-NT_{n+1} (with G on T_{n+2})	ATTAGTATC[n+1] 5′CAGTACGAC ***P***CGCAGCTTGCC NT 3′GTCATGCTGCCCGACCGATGCGTCGAACGG T GGGCUGGC RNA 5′GG	UTP
C/2AP-NT_{n+1}	ATTAGTATC[n+1] 5′CAGTACGAC ***P***CGCAGCTTGCC NT 3′GTCATGCTGCCCGACCGCTGCGTCGAACGG T GGGCUGGC RNA 5′GG	GTP

The 2AP-substituted DNA/RNA elongation substrates are named to indicate the base at position *n* in the T strand followed by the position of 2AP substitution in the T or NT strand. For example, A/2AP-NT_{n+1} contains a dA at T_n and 2AP at $n+1$ in the NT strand (NT_{n+1}).

Changes in steady-state 2AP fluorescence upon binding to T7 RNAP and NTP

The 2AP-modified elongation substrates were analyzed first by measuring their fluorescence intensities after adding T7 RNAP and NTP. Mixing T7 RNAP with the 2AP-modified elongation substrates did not change the fluorescence intensity of 2AP in any of the substrates (Fig. 1a and d). However, fluorescence changes were observed in most cases when a correct NTP was added to the 2AP-modified elongation substrate and T7 RNAP (Fig. 1c and d). The large fluorescence change upon NTP addition to 2AP-NT_{n+1} was abolished when the RNA primer contained a 3′-deoxycytidine (3′-dC) that cannot be elongated (Fig. 1d). The substrate 2AP/2AP-T_n (2AP in the template at *n*-position; Table 1) showed no fluorescence change upon addition of UTP (Fig. 1c). This was surprising as we had expected that 2AP, when placed at the *n*-position, would provide sensitive fluorescence changes because the incoming UTP forms a base pair with 2AP directly and enhances base stacking.[18] Thus, it is difficult to predict simply from the crystal structures the exact sites in the T or the NT strand that will provide large 2AP fluorescence changes upon NTP binding and incorporation.

Fluorescent 2AP in the template strand monitors the kinetics of NMP incorporation

Stopped-flow fluorescence assays were designed to measure the kinetics of single-nucleotide incorporation by T7 RNAP. A preformed complex of C/2AP-T_{n+1} (Table 1) (200 nM) and T7 RNAP (400 nM) was rapidly mixed in a stopped-flow instrument with the correct nucleotide guanosine 5′-triphosphate (GTP) at 1 μM to 400 μM (Fig. 2a). The 2AP fluorescence was recorded from 2 ms to 60 s.[33] A representative time trace of 2AP fluorescence change is shown at 50 μM GTP (Fig. 2c) and fit to a single exponential equation (Eq. 1). The single exponential rate constants (k_{obs}) were plotted against [GTP] (Fig. 2d), and the hyperbolic dependence was fit to Eq. 2 to derive the maximum rate constant of GTP incorporation, $k_{pol} = 190 \pm 10\ s^{-1}$, and the ground-

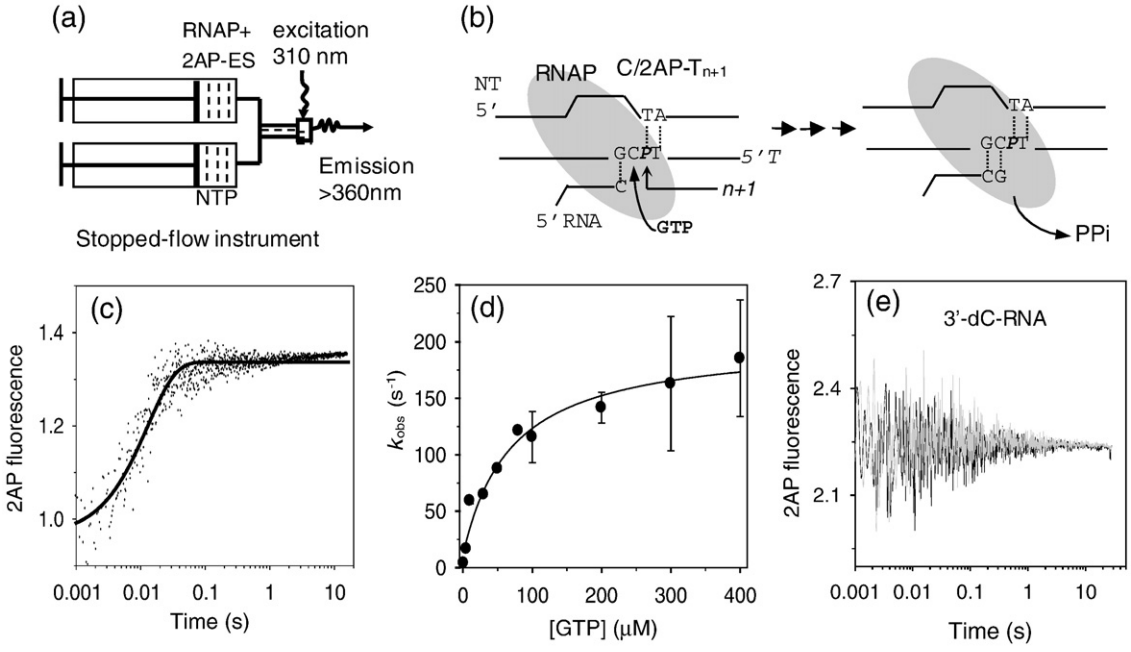

Fig. 2. Elongation substrate with 2AP in the template strand monitors the kinetics of GMP incorporation. (a) The general scheme of the stopped-flow experimental setup consisted of loading a mixture of T7 RNAP (400 nM) and 2AP-labeled elongation substrate (200 nM) in one syringe and NTP in the second syringe. The two solutions were rapidly mixed to initiate the RNA synthesis reaction. The mixed sample was excited with 310-nm light and fluorescence was measured at >360 nm. (b) The elongation substrate (C/2AP-T_{n+1}) contained a 2AP (***P***) in the template strand at $n+1$ position. The C in the template at position *n* will base-pair with GTP. Upon GTP addition, the RNAP moves into the new position where 2AP occupies the *n*-position. (c) Representative time trace at 50 μM GTP shows a single exponential increase (smooth curve) in 2AP fluorescence with $k_{obs} = 77 \pm 4\ s^{-1}$. (d) The GTP concentration dependence of the observed rate constant (k_{obs}) fits to the hyperbolic function (Eq. 2) with a maximum rate constant of $k_{pol} = 190 \pm 10\ s^{-1}$ and a ground-state dissociation constant of $K_d = 70 \pm 10$ μM. Error bars encompass high and low values from duplicate measurements. (e) C/2AP-T_{n+1} substrate with 3′-dC-RNA primer did not show a fluorescence change upon mixing with GTP (200 μM).

Table 2. Kinetic parameters of single correct NTP addition during T7 RNAP elongation

rNTP:template base	k_{pol} (s^{-1})	K_d (μM)	k_{pol}/K_d ($\mu M^{-1}\ s^{-1}$)	Elongation substrate
G:dC	190±10	70±10	2.7	C/2APT$_{n+1}$
3′-dG:dC	45±9	25±4	1.8	
G:dC	178±15	52±17	3.4	C/2AP-NT$_{n+1}$
A:dT	145±5	71±11	2.0	T/2AP-T$_{n+1}$
C:dG	209±27	30±13	7.5	G/2AP-NT$_n$
U:dA	192±20	98±22	2.0	A/2AP-NT$_{n+1}$
	251±23[a]	133±20[a]	1.9[a]	
3′-dU:dA	235±28	185±64	1.3	
U:dA	187±22	124±50	1.5	A/2AP-NT$_{n+1}$ (G-T$_{n+2}$)

[a] From rapid chemical quenched-flow measurements.

state GTP dissociation constant, $K_d = 70 \pm 10$ μM. $k_{pol}/K_d = 2.7\ \mu M^{-1}\ s^{-1}$ is the efficiency of GMP incorporation into RNA during elongation.

To determine whether the increase in 2AP fluorescence was caused by GTP binding or by the GMP incorporation reaction, we substituted the 3′-end of the RNA primer with 3′-dC that lacks the 3′-OH required for polymerization. No fluorescence increase was observed with this 3′-dC elongation substrate upon addition of the correct GTP (Fig. 2e). These results indicate that the observed increase in 2AP fluorescence results from the GMP incorporation step or the following reaction steps.

Changing the template base opposite to the NMP incorporation position (position n) from dC to dT (T/2AP-T$_{n+1}$, Table 1) allowed measurement of AMP incorporation. The analysis indicated that AMP is incorporated into the same RNA primer with $k_{pol} = 145 \pm 5\ s^{-1}$, $K_d = 71 \pm 11$ μM, and $k_{pol}/K_d = 2.0\ \mu M^{-1}\ s^{-1}$ (Table 2).

Fluorescent 2AP in the nontemplate strand monitors the kinetics of NMP incorporation

There is a distinct advantage to having the 2AP probe in the NT strand of the elongation substrate rather than in the T strand. A base analogue in the NT strand is less likely to perturb the nucleotide incorporation kinetics. We therefore investigated the kinetics of nucleotide incorporation with the elongation substrates containing 2AP in the n or $n+1$ position in the NT strand. Addition of the correct CTP to G/2AP-NT$_n$ and T7 RNAP (Fig. 3) resulted in a small increase in 2AP fluorescence, which was monitored as a function of time in the stopped-flow instrument (Fig. 3b). The kinetics fit well to a single exponential equation, and the k_{obs} increased with increasing [CTP] in a hyperbolic manner to provide k_{pol} of $209 \pm 27\ s^{-1}$, K_d of 30±13 μM, and $k_{pol}/K_d = 6.9\ \mu M^{-1}\ s^{-1}$ (Fig. 3c).

When similar experiments were carried out with A/2AP-NT$_{n+1}$, where UTP is the correct nucleotide

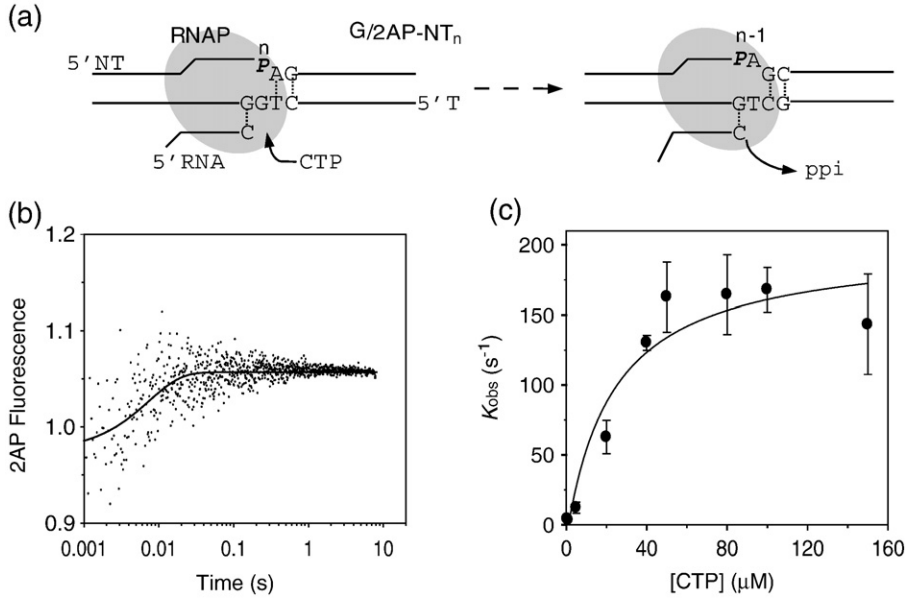

Fig. 3. Elongation substrate with 2AP in the nontemplate strand monitors the kinetics of CMP incorporation. (a) The G/2AP-NT$_n$ elongation substrate contains a 2AP in the NT at the n-position and correctly base-pairs with CTP. (b) A representative time trace of 2AP fluorescence change at 40 mM CTP (200 nM G/2AP-NT$_n$) and 400 nM T7 RNAP). The experimental data fit well to a single exponential equation (Eq. 1) (continuous line) with $k_{obs} = 136 \pm 24\ s^{-1}$. (d) The k_{obs} increased with increasing [CTP] and fit to the hyperbola (Eq. 2) with a maximum rate constant of $k_{pol} = 209 \pm 27\ s^{-1}$ and $K_d = 28 \pm 13$ μM. Error bars indicate the high and low values from duplicate measurements.

to be added (Fig. 4a), two phases of fluorescence changes were observed. Four representative time traces of 2AP fluorescence changes at selected [UTP] are shown in Fig. 4b. At low UTP concentrations (1 μM), the time-dependent 2AP fluorescence change fit well to a single exponential equation. Above 5 μM, the kinetics fit to the sum of two exponentials. The fast increase in 2AP fluorescence was followed by a 200-fold slower increase (Fig. 4b).

The observed rate constants for the fast and slow phases, $k_{obs\text{-}1}$ and $k_{obs\text{-}2}$, and their corresponding amplitudes of 2AP fluorescence changes were plotted against [UTP] (Fig. 4b–d). $k_{obs\text{-}1}$ increased with [UTP] in a hyperbolic manner, providing a maximal rate constant of $k_{pol\text{-}1}=192\pm20\ s^{-1}$, $K_{d\text{-}1}=98\pm22$ μM, and $k_{pol}/K_d=2.0\ \mu M^{-1}\ s^{-1}$. These kinetic parameters are very close to those measured for other correct NTP addition reactions, as described above. The amplitude of the fast fluorescence change saturated after 5 μM UTP (Fig. 4d), demonstrating a tight net binding affinity of UTP ($K_{d\text{-}net1}\sim0.5$ μM) resulting from forward favorable steps of chemistry and product release beyond the collision complex with UTP [$K_{d\text{-}net1}=K_{d\text{-}1}/(1+K_2+K_2K_3)$, K_2 and K_3 are the equilibrium constants of conformational change and chemistry].[34]

The rate constant of the slow phase ($k_{obs\text{-}2}$) increased with [UTP] linearly with slope=0.0018

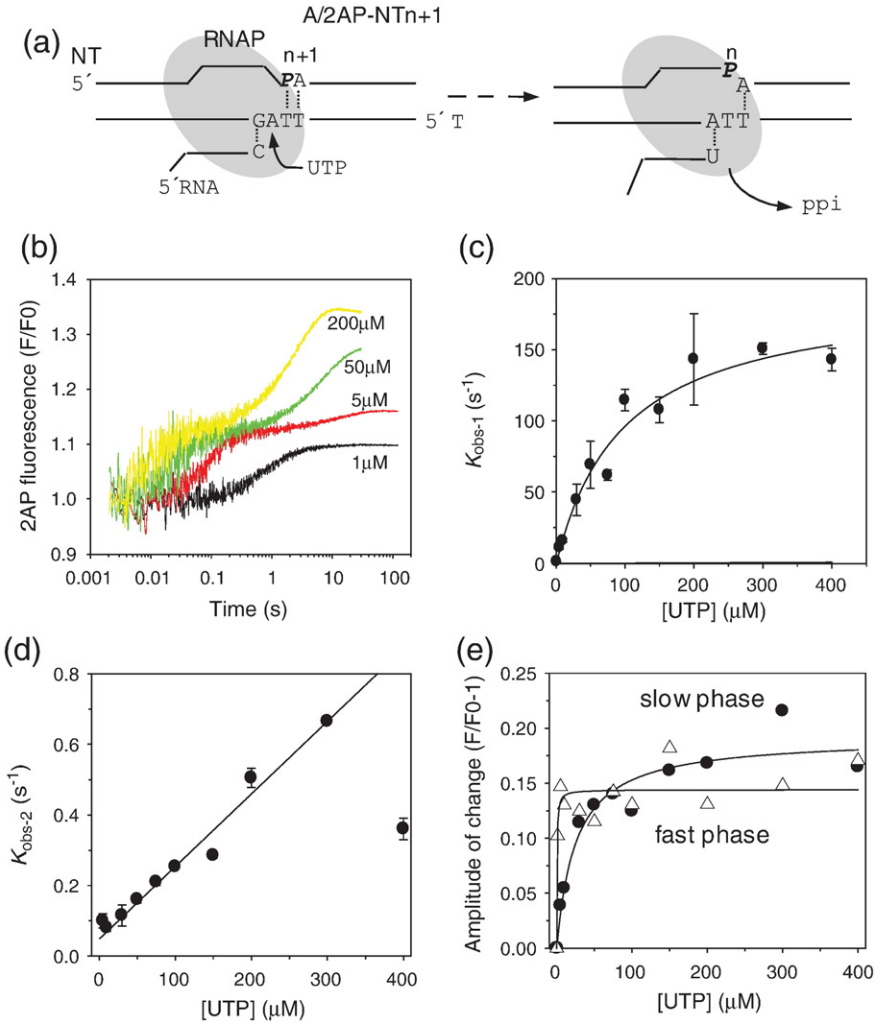

Fig. 4. Stopped-flow kinetics of multiple UMP incorporation. (a) The A/2AP-NT$_{n+1}$ contains 2AP in the NT strand at $n+1$ position and correctly base-pairs with UTP. (b) Representative time traces of 2AP fluorescence changes upon adding UTP (1, 5, 50, and 200 mM final concentrations) show multiple kinetic phases. (c) The $k_{obs\text{-}1}$ of the fast phase increases with [UTP] in a hyperbolic manner with $k_{pol\text{-}1}=192\pm20\ s^{-1}$ and $K_{d\text{-}1}=98\pm22$ μM. Error bars indicate SD from multiple measurements. (d) The UTP concentration dependence of the slow-phase $k_{obs\text{-}2}$ shows a linear dependence, with slope=0.002 $\mu M^{-1}\ s^{-1}$ representing the $k_{pol\text{-}2}/K_{d\text{-}2}$ ratio. The UTP concentration dependence of the fast-phase (open triangle) and slow-phase (filled circle) amplitudes of 2AP fluorescence changes fits to the hyperbolic equation (Eq. 2) with $K_{d,net}=0.3$ μM for correct UMP:dA incorporation and $K_{d,net2}=32$ μM for UMP:dA misincorporation.

μM^{-1} s^{-1} (Fig. 5c). Since $k_{obs\text{-}2}$ did not saturate in the range of [UTP] examined, we could not obtain the individual $k_{pol\text{-}2}$ and $K_{d\text{-}2}$ values. However, the slope represents the $k_{pol\text{-}2}/K_{d\text{-}2}$ ratio, which was 1000-fold slower than the $k_{pol\text{-}1}/K_{d\text{-}1}$ ratio of the first phase ($192/98 = 1.96$ μM^{-1} s^{-1}). The amplitude of the second phase increased hyperbolically with increasing [UTP] as compared to the first phase and indicates a 60-fold weaker net dissociation constant, $K_{d\text{-}net2} = 32$ μM.

We hypothesized that the second slow phase observed at >5 μM UTP at extended reaction times arises from the misincorporation of UMP. To test this hypothesis, we used 3′-dUTP as the nucleotide substrate instead of UTP to stop synthesis after one nucleotide addition (Fig. 5a). Consistent with our hypothesis, only a single fast phase of 2AP fluorescence increase was observed upon addition of 3′-dUTP (Fig. 5b). As compared to UTP, 3′-dUTP binds with a 2-fold weaker affinity with $K_d = 185 \pm 64$ μM and is incorporated with a maximum rate constant of $k_{pol} = 235 \pm 28$ s^{-1} and $k_{pol}/K_d = 1.3$ μM^{-1} s^{-1} (Fig. 5c), which is similar to UMP incorporation. The amplitude of 2AP fluorescence change was also 20–40% of the change observed after UTP additions and saturation, yielding a tight net binding with $K_{d,\ net} \sim 5$ μM.

When experiments were conducted with a mixture of UTP and ATP that can correctly base-pair to n, $n+1$, and $n+2$ of the A/2AP-NT_{n+1} substrate (Fig. 5d), the initial fast phase remained unchanged, but the slower phase was replaced by a faster phase

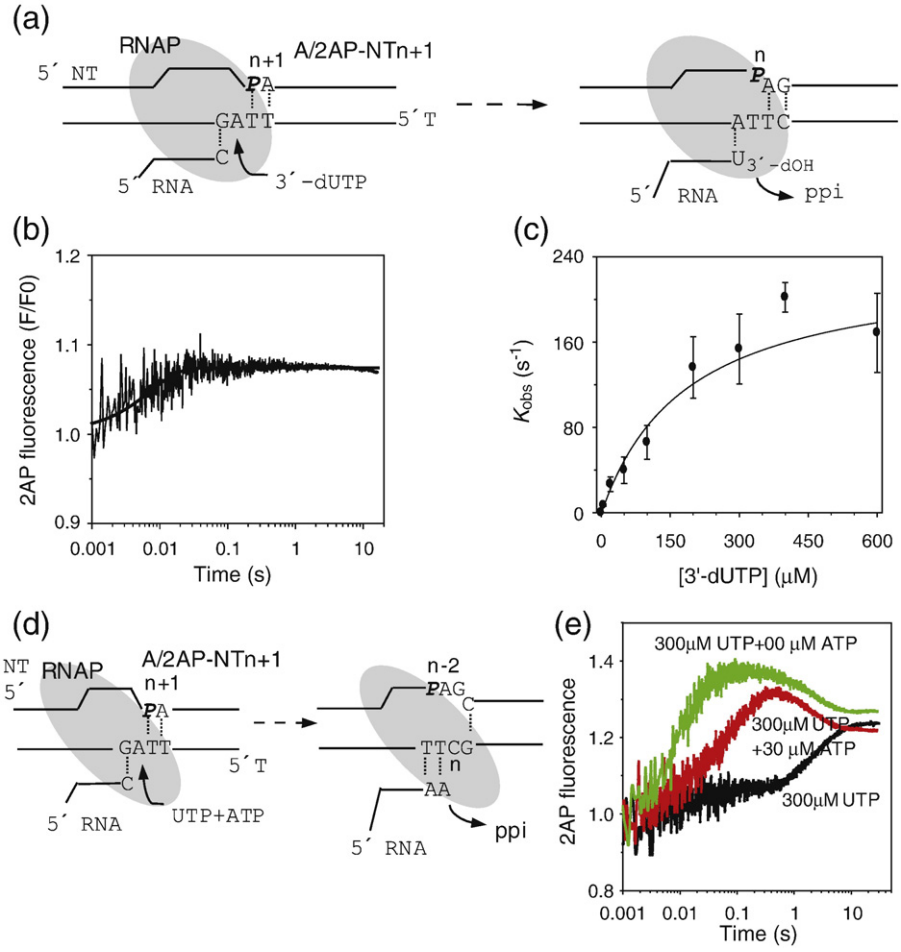

Fig. 5. Fluorescence measurements supporting the slow phase of UMP:dA misincorporation. (a) Measurement of 3′-dUMP incorporation in A/2AP-NT_{n+1}. (b) A representative time course of 2AP fluorescence change at 50 mM 3′-dUTP fits to a single exponential $k_{obs} = 39$ s^{-1}. (c) The 3′-dUTP concentration dependence of k_{obs} fits to the hyperbola with $k_{pol} = 235 \pm 28$ s^{-1} and $K_d = 185 \pm 64$ μM. Error bars encompass the high and low values from duplicate measurements. (d) Measurement of successive UMP and AMP incorporation in A/2AP-NT_{n+1}. (e) Representative time traces show multiple 2AP fluorescence changes with 300 μM UTP alone (black trace), UTP + 30 μM ATP (red trace), and UTP + 300 μM ATP (green trace).

(Fig. 5e). In addition, a late time period fluorescence decrease was observed that brought the fluorescence intensity back to the same level of adding UTP alone. This is consistent with the changes measured under steady-state conditions with UTP and UTP + ATP (Fig. 1d). The fluorescence decrease occurred with a rate constant (0.4–0.5 s^{-1}) that is equal to the UMP misincorporation reaction at 300 μM UTP, suggesting that the decrease in fluorescence monitors the UMP misincorporation reaction opposite C at $n+3$ after correct UMP and AMP incorporations. These results indicate that multiple RNA extension cycles can be measured by following 2AP fluorescence changes in modified elongation substrates.

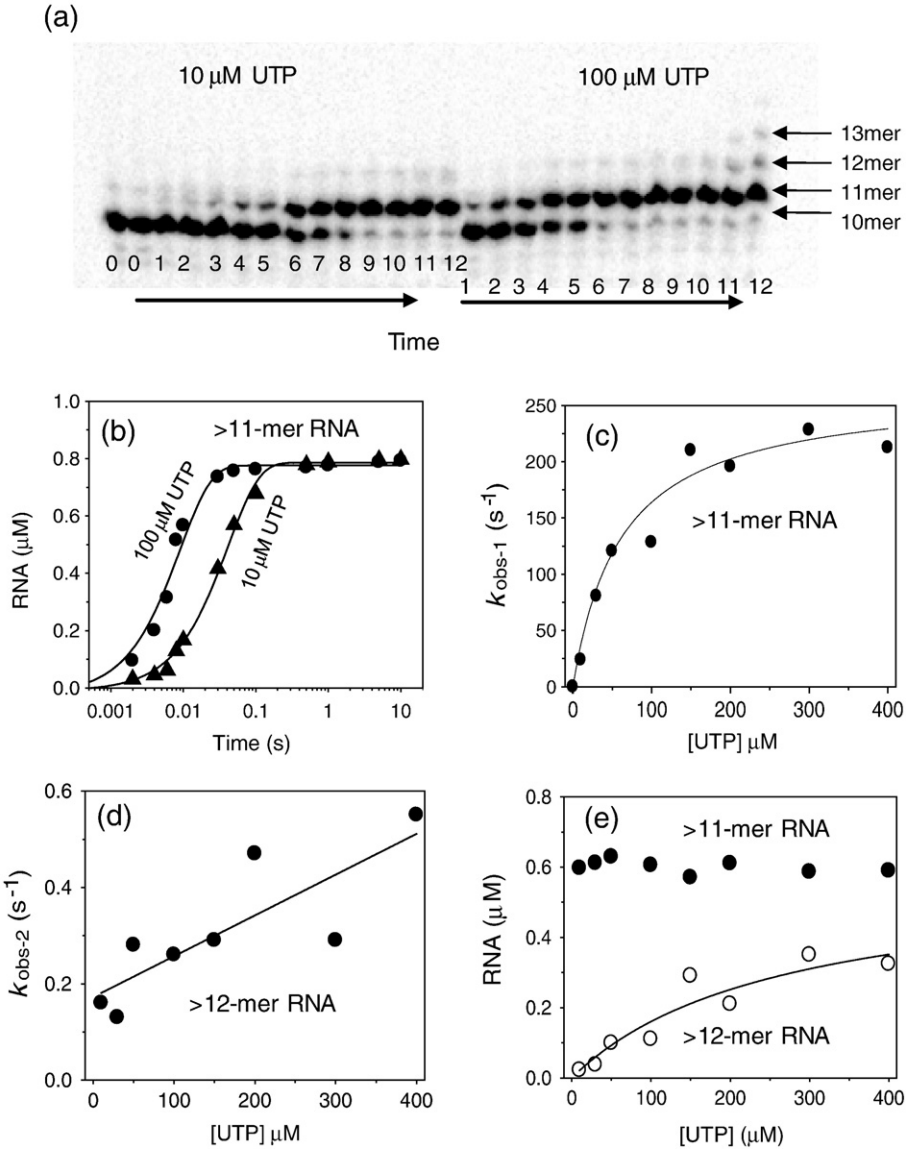

Fig. 6. UMP incorporation during RNA synthesis measured by the radiometric assay. (a) The polyacrylamide sequencing gels show the 10-mer RNA elongated to 11- to 13-mer RNAs with increasing reaction times. Lanes 0–12 represent reaction times from 0, 2, 4, 6, 8, 10, 30, 50, 100, and 500 ms and 1, 5, and 10 s, respectively, at 10 mM (left side) or 100 mM (right side) UTP. (b) The kinetics of 11- to 13-mer RNA formation at UTP concentrations of 10 mM (filled circles) and 100 mM (filled triangles) were fit to a single exponential equation (Eq. 1) with $k_{obs} = 24\ s^{-1}$ and $113\ s^{-1}$, respectively. (c) The UTP concentration dependence of k_{obs} for correct UMP incorporation fits to the hyperbolic function (Eq. 2) with $k_{pol} = 251 \pm 23\ s^{-1}$ and $K_d = 133 \pm 20$ μM. (d) The UTP concentration dependence of the k_{obs} for rU:dA misincorporation fits to a line with slope = 0.001 $\mu M^{-1}\ s^{-1}$. (e) UTP concentration dependence of the amplitudes of correct (filled circle) and incorrect (open circle) UMP incorporation. A net dissociation constant for UMP misincorporation ($K_{d,net-mis} = 263$ μM) was derived from the hyperbolic fitting.

Kinetics of UTP incorporation by radiometric quenched-flow assay

The complex kinetics of UMP incorporation in the 2AP-NT$_{n+1}$ substrate was further investigated by the radiometric assay of transcription elongation.[13] The time course of extension of the ^{32}P-labeled 10-mer RNA primer in the NT$_{n+1}$ elongation substrate was measured at various [UTP], from 10 to 400 μM. A representative sequencing gel at 10 or 100 μM UTP (Fig. 6a) shows the starting RNA 10-mer to be elongated to the major product 11-mer RNA after a single UMP incorporation reaction. In addition to the major 11-mer RNA product, we observed 12-mer and 13-mer RNAs after longer reaction times (>1 s) and at higher UTP concentrations (>10 μM UTP). These longer RNA products are made by successive events of UMP misincorporation to the 11-mer RNA.

The kinetics of correct UMP addition was determined by plotting the amount of total RNA at each [UTP] as a function of time (Fig. 6b). The kinetics of incorrect UMP addition was determined by plotting >11-mer RNA at each [UTP] as a function of time (Fig. 6b). Each of the kinetics was fit to a single exponential equation (Eq. 1) to determine the rate constants for correct (k_{obs-1}) (Fig. 6c) and incorrect (k_{obs-2}) UMP additions (Fig. 6d). The k_{obs1} of correct addition *versus* [UTP] fit to the hyperbolic equation (Eq. 2) with $k_{pol\ -1} = 251 \pm 23\ s^{-1}$, UTP $K_{d-1} = 133 \pm 20$ μM, and $k_{pol}/K_d = 1.9\ \mu M^{-1}\ s^{-1}$, consistent with the values for correct UMP addition from the stopped-flow fluorescence assay described above (Fig. 4c). The [UTP] dependence of k_{obs-2}, the rate constant of incorrect UMP addition, did not reach saturation. Linear fitting yielded a k_{pol-2}/K_{d-2} $\sim 0.001\ \mu M^{-1}\ s^{-1}$ for rUMP:dT misincorporation (Fig. 6d). This value is consistent with the k_{pol}/K_d of the second slow phase in the fluorescence-based assay, as described above (Fig. 4d).

The amount of 11-mer RNA product after reaction completion was largely constant from 10 to 400 μM UTP (Fig. 6e), which is consistent with the amplitudes of the fluorescence-based assay (Fig. 4f). The amount of >11-mer RNA after reaction completion depended on [UTP] (Fig. 6e) and increased in a hyperbolic manner, yielding a net $K_{d\text{-}net2} = 263$ μM. These radiometric assays confirm that the second slow phase in the fluorescence-based assay is due to UMP misincorporation reactions. Thus, the fluorescence-based assay provides a fast and sensitive means to measure both correct and incorrect NTP addition reactions of T7 RNAP.

Measurement of the nucleotide misincorporation kinetics

Next, we measured the kinetics of nucleotide misincorporation directly using the fluorescence-based stopped-flow assay. The T/2AP-T$_{n+1}$ (Table 1) elongation substrate contains a dT at the *n*-position (Fig. 7a) and adds the correct ATP at a rapid rate. To measure misincorporation, we added GTP to the reactions and observed a large fluorescence increase albeit at a slower rate (Fig. 7b). The 2AP fluorescence increase with GTP reached approximately 60% of the level observed with the correct ATP (Fig. 7b). Fitting the GTP concentration dependence of the observed rate constants, k_{obs}, to the hyperbolic equation revealed a maximum rate constant of $k_{pol} = 5.2\ s^{-1}$ for GMP misincorporation against dT, $K_d = 1.8$ mM, and k_{pol}/

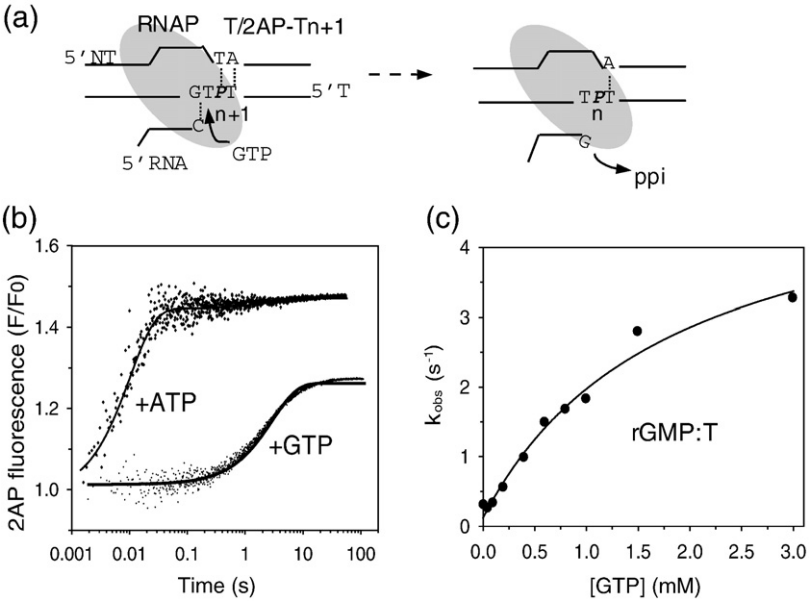

Fig. 7. Stopped-flow fluorescence measurements of G:dT misincorporation. (a) Addition of GTP to T/2AP-T results in rG:dT misincorporation. (b) Representative time traces of correct and incorrect NTP addition. 2AP fluorescence increases upon addition of the incorrect GTP (200 mM) with $k_{obs} = 0.6\ s^{-1}$ and of the correct ATP (200 mM) with $k_{obs} = 100\ s^{-1}$. (b) The GTP concentration dependence of the misincorporation reaction rate constant fits to the hyperbola (Eq. 2) with $k_{pol} = 5.2 \pm 0.6\ s^{-1}$ and $K_d = 1816 \pm 483$ μM.

Table 3. Kinetic parameters for single incorrect NTP addition during T7 RNAP elongation

rNTP:template	k_{pol} (s^{-1})	K_d (μM)	k_{pol}/K_d (μM^{-1} s^{-1})	Discrimination[a]	Elongation substrate
U:dT			0.001, 0.002[b]	2000, 1000	A/2AP-NT_{n+1}[c]
			0.0015	1333	A/2AP-NT_{n+1}[c] (G-T_{n+2})
G:dT	5.2±0.6	1816±483	0.0029	690	T/2AP
	6.9±0.7	3864±754	0.0018	1111	C/2AP

[a] Discrimination is calculated from $(k_{pol}/K_d)_{correct}/(k_{pol}/K_d)_{incorrect}$.
[b] From rapid chemical quenched-flow measurements.
[c] From the slow phase of fluorescence change following the fast correct incorporation.

$K_d = 0.0029$ μM^{-1} s^{-1} (Fig. 7c). Compared to the correct nucleotide ATP, the incorrect GTP binds ~25-fold more weakly and is incorporated with ~30-fold slower rate (Table 3). The results indicate that T7 RNAP discriminates against G:dT mismatch by ~720-fold $[(k_{pol}/K_d)_{ATP}/(k_{pol}/K_d)_{GTP}]$, both by slower catalysis and by weaker binding to the incorrect NTP. The kinetics of both correct and incorrect GMP incorporation was measured using the C/2AP-NT_{n+1} substrate in one experiment that showed two phases, whose rates increased with increasing [GTP]. The rate of the fast phase provided $k_{pol} = 178$ s^{-1}, $K_d = 52$ μM, and $k_{pol}/K_d = 3.4$ μM^{-1} s^{-1} for correct GMP incorporation (Table 2), and the rate of the slow phase provided $k_{pol} = 6.9$ s^{-1}, $K_d = 3.9$ mM, and $k_{pol}/K_d = 0.0018$ μM^{-1} s^{-1} for the rGMP:dT misincorporation reaction (Table 3).

Discussion

We report a fluorescence-based assay that measures the pre-steady-state kinetics of single-nucleotide addition by T7 RNAP during the transcription elongation phase. This assay was developed using 2AP, a fluorescent adenine analogue, whose fluorescence intensity is sensitive to base stacking–unstacking changes in DNA. Through experimentation, we have identified several positions in the elongation substrate that, when modified with a single 2AP, provide robust fluorescence changes for real-time measurement of the kinetics of correct and incorrect nucleotide addition. Although the 2AP-based assay has been used to dissect the kinetic pathway of DNA polymerases[26–29], such high-throughput fluorescence-based assays are not able to measure the kinetics of single-nucleotide addition by the DNA-dependent RNAPs.

K_d and k_{pol} are the two parameters that provide a quantitative measure of nucleotide affinity and incorporation into RNA. To obtain these parameters, the single turnover rates of nucleotide addition to the RNA are measured as a function of [NTP]. T7 RNAP assembles as an elongation complex on a synthetic substrate that contains an 8-bp RNA:DNA hybrid in a preformed transcription elongation bubble.[16] A single 2AP was incorporated in these elongation substrates, either in the T or the NT strand of the DNA. In our synthetic mismatched elongation substrate, as RNA is synthesized, the upstream bases cannot reanneal. Thus, there is a concern that the measured rates of correct and incorrect nucleotide addition might be different from those with the matched substrate. We believe that this is less of a concern in our studies because we are measuring the kinetics of single-nucleotide incorporation, and RNA polymerases including T7 RNAP are competent in adding multiple nucleotides on mismatched elongation substrates.[16,19,20] The 2AP-based approach can be applied to matched elongation substrates in future experiments to address this issue. We attempted to make predictions based on the available high-resolution structures of the elongation complexes of T7 RNAP as to which position undergoes large stacking–unstacking changes upon nucleotide addition. However, contrary to our expectations (e.g., when 2AP was introduced at T_n), no measurable fluorescence change was observed (n is the position where the incoming NTP will base-pair). 2AP placed in the n-position in the primer/template substrates provides large fluorescence changes that have been used to measure the kinetics of DNA synthesis.[26–28] We therefore chose a scanning approach, wherein we experimentally tested several positions for 2AP incorporation around the site of nucleotide incorporation.

The substrates with a single 2AP at NT_{n+1}, NT_n, or T_{n+1} served as excellent fluorescent elongation substrates. The fluorescence intensities of these substrates showed an increase with the addition of the correct NTP to the RNA. Using 3′-deoxy RNA substrates, we showed that the fluorescence changes do not result from the NTP binding steps. We propose that the observed 2AP fluorescence changes arise from the chemical step or the PPi release/translocation step. From the kinetics of fluorescence change at various [NTP], we determined the k_{pol} and K_d of all four correct NTP addition reactions by T7 RNAP (Table 2). We found that the k_{pol} of correct nucleotide addition ranges from 145 to 190 s^{-1} and the K_d ranges from of 28 to 124 μM. The range of values indicates that nucleotide incorporation efficiency depends on the NTP added and the surrounding DNA sequence. Additional studies will be necessary to understand the sequence context of transcription efficiency.

The values from the fluorescence assay are consistent with the reported k_{pol} and K_d of UTP addition opposite dA from the radiometry-based rapid quenched-flow assay[13] and those measured here using radiometric assays. Thus, the two assays, fluorescence-based stopped-flow and radiometric-based quenched-flow, measure the same rate-limiting step. Previous studies have shown that the single-nucleotide incorporation reaction by T7 RNAP is rate limited either by the open-to-closed conformational transition of the enzyme upon NTP binding or by the chemical step, while PPi release and the coupled translocation were proposed to be faster.[13] Because we expect larger structural changes in the elongation substrate from the translocation step rather than the chemical step, we propose that the 2AP fluorescence changes are arising from steps after chemistry. In future studies, we hope to develop substrates that will measure the NTP binding steps.

The elongation substrate with 2AP at NT_{n+1} showed two phases upon nucleotide addition (UTP to A/2AP-NT_{n+1} or GTP to C/2AP-NT_{n+1}). Using several experiments, we verified that the fast phase was due to correct UTP addition against dA in the template and the slow phase was due to misincorporation extension. The ability to resolve the fast and slow phases allows correct and incorrect misincorporation kinetics to be measured simultaneously in a single experiment, providing a powerful assay to investigate the misincorporation kinetics sensitive to sequence context.[15] We used some of the fluorescent elongation substrates to measure the misincorporation kinetics directly by adding an incorrect NTP instead of the correct one. These studies investigated the G:dT misincorporation reaction and showed that the incorrect GTP is added with 30- to 40-fold slower k_{pol} as compared to the correct nucleotide, and the incorrect GTP K_d is 25–100 times greater than that of the correct NTP. This indicates that T7 RNAP discriminates against the incorrect NTP both at the binding and nucleotide incorporation steps. The k_{pol}/K_d ratios of correct and incorrect nucleotide addition indicate that T7 RNAP discriminates against incorrect GTP addition ~1000-fold as compared to correct GTP addition. These studies indicate that the fluorescence-based assay is a highly suitable method for determining the misincorporation kinetics of a complete set of NTPs under various DNA:RNA sequence contexts. Such studies in the future with other misincorporations will be required to fully understand the fidelity of RNAP-catalyzed transcription elongation reactions. The elongation substrate with 2AP at T_{n+1} also showed a slow phase of 2AP fluorescence change, but the amplitude was not significant to allow accurate measurement of the misincorporation reaction (Figs. 2c and 7b). The much reduced amplitude was partly due to the insensitivity of 2AP at T_n after it was translocated from T_{n+1}. Hence, while 2AP at NT_{n+1}, NT_n, or T_{n+1} can be used to separately measure correct and incorrect nucleotide incorporation, only 2AP at NT_{n+1} is optimal for simultaneously measuring both reactions in a single kinetic experiment.

In summary, the fluorescence-based RNA synthesis assay provides a quick and sensitive means to study the kinetics of single-nucleotide incorporation and misincorporation during RNA elongation. The advantage of the fluorescence-based assay is the speed and the ability to measure RNA synthesis in real time that will allow high-throughput analysis of sequence dependence of transcription. The RNAPs from phage to eucaryotes, despite having different structures and subunit composition, use similar RNA:DNA elongation substrates.[16,19,20,31,32] The fluorescent elongation substrates should therefore serve as general substrates for all DNA-dependent RNAPs to study single-nucleotide incorporation kinetics with high time resolution. Potentially, these substrates can be used to measure the kinetics of a specific step in the pathway of single-nucleotide incorporation, thus helping to dissect the complex multistep elongation process. The assay can be used as a fast means of screening RNAP variants, nucleotide analogues, and small chemical inhibitors of RNA synthesis.

Materials and Methods

Nucleic acids, T7 RNAP, and other reagents

Untagged T7 RNAP was overexpressed in *Escherichia coli* strain BL21 and purified as described previously.[4] Oligodeoxynucleotides (Table 1) were custom synthesized from IDT (Coralville, IA) and purified on a 14% polyacrylamide/urea gel. PAGE-purified RNA was purchased from Dharmacon Research Inc. (Lafayette, CO), which was 2′-deprotected/desalted before use. In rapid chemical quench-flow assay, RNA was radiolabeled at the 5′ terminus using γ-^{32}P-ATP and polynucleotide kinase. Unlabeled isotope was removed by Sephadex G50 gel filtration. The elongation substrate was assembled by mixing the template strand (T), nontemplate DNA (NT), and 5′-^{32}P-labeled or unlabeled RNA in a 1:1.5:1 ratio in transcription buffer at a final concentration of 20 μM, which was then heated at 95 °C for 5 min and slowly cooled to 4 °C for 2 h. The transcription buffer consisted of 50 mM Tris acetate (pH 7.5), 50 mM sodium acetate, 10 mM magnesium acetate, and fresh 2 mM dithiothreitol.

Stopped-flow fluorescence experiments

A mixture of 200 nM 2AP-labeled elongation substrate and 400 nM T7 RNAP in transcription buffer was loaded in one syringe of the stopped-flow instrument and UTP was loaded in the other syringe. The two solutions were rapidly mixed at 25 °C, and 2AP fluorescence (using 370-nm long-

pass filter) was measured in real time after excitation at 310 nm.[33] The kinetics of fluorescence increase was measured at various [NTP], ranging from 1 to 400 μM, and fit to single or double exponential equation:

$$F_t = F_0 + \Sigma(1 - A)e^{-k_{obs}t} \quad (1)$$

where F_0 and F_t are the 2AP fluorescence intensity at time (t) zero, A is the amplitude of fluorescence change, and k_{obs} is the observed rate constant. The observed rate constant, k_{obs}, was plotted as a function of [NTP] and fit to Eq. 2:

$$k_{obs} = k_{pol}[NTP] / (K_d + [NTP]) \quad (2)$$

where K_d is the ground-state dissociation constant of the NTP upon binding to the T7 RNAP–elongation substrate complex, and k_{pol} is the maximum rate constant of NMP incorporation measured by 2AP fluorescence changes or radiometry.

Rapid chemical quench-flow experiments

Pre-steady-state kinetic experiments were performed at 25 °C using a chemical quench-flow apparatus (model RQF-3, KinTek Corp., Austin, TX).[13] The preformed complex of T7 RNAP–elongation substrate (1.5 mM:0.75 mM, final) with 5′-^{32}P-labeled RNA from syringe A was rapidly mixed with UTP (10–400 mM) from syringe B to initiate RNA synthesis. The reaction was terminated by mixing with 200 mM EDTA from syringe C after predefined time intervals. RNA products were resolved on a 7 M urea-denatured sequencing gel consisting of 20% polyacrylamide–1.5% bis-acrylamide. RNA was quantified on a Typhoon 9410 PhosphorImager (Amersham Biosciences) using the ImageQuaNT software (GE Healthcare). The fraction of RNA primers converted to products was determined from the ratio of their respective counts to the total counts, and the concentration of the product was determined by multiplying the fraction with the concentration of the RNA primer. The kinetics was fit to Eq. 1, where F_t is the fraction or molar amount of products, F_0 is the y-intercept or background, A is the amplitude or the total amount of products formed during the reaction, and k_{obs} is the observed rate constant of product formation. The observed rate, k_{obs}, plotted as a function of [NTP], was fit to Eq. 2 to derive the maximum rate constant of NMP incorporation, k_{pol}, and the apparent dissociation constant, K_d.

Acknowledgement

This work was supported by a NIH grant (GM51966) to S.S.P.

References

1. Gralla, J. D., Carpousis, A. J. & Stefano, J. E. (1980). Productive and abortive initiation of transcription *in vitro* at the lac UV5 promoter. *Biochemistry*, **19**, 5864–5869.
2. Martin, C. T., Muller, D. K. & Coleman, J. E. (1988). Processivity in early stages of transcription by T7 RNA polymerase. *Biochemistry*, **27**, 3966–3974.
3. Villemain, J., Guajardo, R. & Sousa, R. (1997). Role of open complex instability in kinetic promoter selection by bacteriophage T7 RNA polymerase. *J. Mol. Biol.* **273**, 958–977.
4. Jia, Y. & Patel, S. S. (1997). Kinetic mechanism of transcription initiation by bacteriophage T7 RNA polymerase. *Biochemistry*, **36**, 4223–4232.
5. Hsu, L. M. (2002). Promoter clearance and escape in prokaryotes. *Biochim. Biophys. Acta*, **1577**, 191–207.
6. Tang, G. Q., Roy, R., Bandwar, R. P., Ha, T. & Patel, S. S. (2009). Real-time observation of the transition from transcription initiation to elongation of the RNA polymerase. *Proc. Natl Acad. Sci. USA*, **106**, 22175–22180.
7. Johnson, K. A. (1993). Conformational coupling in DNA polymerase fidelity. *Annu. Rev. Biochem.* **62**, 685–713.
8. Kunkel, T. A. & Bebenek, K. (2000). DNA replication fidelity. *Annu. Rev. Biochem.* **69**, 497–529.
9. Joyce, C. M. & Benkovic, S. J. (2004). DNA polymerase fidelity: kinetics, structure, and checkpoints. *Biochemistry*, **43**, 14317–14324.
10. Johnson, K. A. (2010). The kinetic and chemical mechanism of high-fidelity DNA polymerases. *Biochim. Biophys. Acta*, **1804**, 1041–1048.
11. Foster, J. E., Holmes, S. F. & Erie, D. A. (2001). Allosteric binding of nucleoside triphosphates to RNA polymerase regulates transcription elongation. *Cell*, **106**, 243–252.
12. Nedialkov, Y. A., Gong, X. Q., Hovde, S. L., Yamaguchi, Y., Handa, H., Geiger, J. H. *et al.* (2003). NTP-driven translocation by human RNA polymerase II. *J. Biol. Chem.* **278**, 18303–18312.
13. Anand, V. S. & Patel, S. S. (2006). Transient state kinetics of transcription elongation by T7 RNA polymerase. *J. Biol. Chem.* **281**, 35677–35685.
14. Holmes, S. F., Santangelo, T. J., Cunningham, C. K., Roberts, J. W. & Erie, D. A. (2006). Kinetic investigation of *Escherichia coli* RNA polymerase mutants that influence nucleotide discrimination and transcription fidelity. *J. Biol. Chem.* **281**, 18677–18683.
15. Huang, J., Brieba, L. G. & Sousa, R (2000). Misincorporation by wild-type and mutant T7 RNA polymerases: identification of interactions that reduce misincorporation rates by stabilizing the catalytically incompetent open conformation. *Biochemistry*, **39**, 11571–11580.
16. Temiakov, D., Anikin, M. & McAllister, W. T. (2002). Characterization of T7 RNA polymerase transcription complexes assembled on nucleic acid scaffolds. *J. Biol. Chem.* **277**, 47035–47043.
17. Tahirov, T. H., Temiakov, D., Anikin, M., Patlan, V., McAllister, W. T., Vassylyev, D. G. & Yokoyama, S. (2002). Structure of a T7 RNA polymerase elongation complex at 2.9 A resolution. *Nature*, **420**, 43–50.
18. Yin, Y. W. & Steitz, T. A. (2002). Structural basis for the transition from initiation to elongation transcription in T7 RNA polymerase. *Science*, **298**, 1387–1395.

19. Sidorenkov, I., Komissarova, N. & Kashlev, M. (1998). Crucial role of the RNA:DNA hybrid in the processivity of transcription. *Mol. Cell*, **2**, 55–64.
20. Daube, S. S. & von Hippel, P. H. (1992). Functional transcription elongation complexes from synthetic RNA–DNA bubble duplexes. *Science*, **258**, 1320–1324.
21. Kireeva, M., Nedialkov, Y. A., Gong, X. Q., Zhang, C., Xiong, Y., Moon, W. *et al.* (2009). Millisecond phase kinetic analysis of elongation catalyzed by human, yeast, and *Escherichia coli* RNA polymerase. *Methods*, **48**, 333–345.
22. Ujvari, A. & Martin, C. T. (1996). Thermodynamic and kinetic measurements of promoter binding by T7 RNA polymerase. *Biochemistry*, **35**, 14574–14582.
23. Jia, Y. & Patel, S. S. (1997). Kinetic mechanism of GTP binding and RNA synthesis during transcription initiation by bacteriophage T7 RNA polymerase. *J. Biol. Chem.* **272**, 30147–30153.
24. Bandwar, R. P. & Patel, S. S. (2001). Peculiar 2-aminopurine fluorescence monitors the dynamics of open complex formation by bacteriophage T7 RNA polymerase. *J. Biol. Chem.* **276**, 14075–14082.
25. Frey, M. W., Sowers, L. C., Millar, D. P. & Benkovic, S. J. (1995). The nucleotide analog 2-aminopurine as a spectroscopic probe of nucleotide incorporation by the Klenow fragment of *Escherichia coli* polymerase I and bacteriophage T4 DNA polymerase. *Biochemistry*, **34**, 9185–9192.
26. Dunlap, C. A. & Tsai, M. D. (2002). Use of 2-aminopurine and tryptophan fluorescence as probes in kinetic analyses of DNA polymerase beta. *Biochemistry*, **41**, 11226–11235.
27. Fidalgo da Silva, E., Mandal, S. S. & Reha-Krantz, L. J. (2002). Using 2-aminopurine fluorescence to measure incorporation of incorrect nucleotides by wild type and mutant bacteriophage T4 DNA polymerases. *J. Biol. Chem.* **277**, 40640–40649.
28. Purohit, V., Grindley, N. D. & Joyce, C. M. (2003). Use of 2-aminopurine fluorescence to examine conformational changes during nucleotide incorporation by DNA polymerase I (Klenow fragment). *Biochemistry*, **42**, 10200–10211.
29. Zhang, H., Cao, W., Zakharova, E., Konigsberg, W. & De La Cruz, E. M. (2007). Fluorescence of 2-aminopurine reveals rapid conformational changes in the RB69 DNA polymerase-primer/template complexes upon binding and incorporation of matched deoxynucleoside triphosphates. *Nucleic Acids Res.* **35**, 6052–6062.
30. Datta, K., Johnson, N. P. & von Hippel, P. H. (2006). Mapping the conformation of the nucleic acid framework of the T7 RNA polymerase elongation complex in solution using low-energy CD and fluorescence spectroscopy. *J. Mol. Biol.* **360**, 800–813.
31. Daube, S. S. & von Hippel, P. H. (1994). RNA displacement pathways during transcription from synthetic RNA–DNA bubble duplexes. *Biochemistry*, **33**, 340–347.
32. Kashkina, E., Anikin, M., Tahirov, T. H., Kochetkov, S. N., Vassylyev, D. G. & Temiakov, D. (2006). Elongation complexes of *Thermus thermophilus* RNA polymerase that possess distinct translocation conformations. *Nucleic Acids Res.* **34**, 4036–4045.
33. Tang, G. Q. & Patel, S. S. (2006). Rapid binding of T7 RNA polymerase is followed by simultaneous bending and opening of the promoter DNA. *Biochemistry*, **45**, 4947–4956.
34. Tsai, Y. C. & Johnson, K. A. (2006). A new paradigm for DNA polymerase specificity. *Biochemistry*, **45**, 9675–9687.